

**DESIGN AND IMPLEMENTATION OF A SYSTEM FOR
RAPID INSPECTION OF CRITICAL DIMENSIONS
IN HIGH VOLUME PRODUCTION**

Christopher T. Gallagher

The Timken Company
Canton, Ohio

Thomas R. Kurfess

The George W. Woodruff School of Mechanical Engineering
Georgia Institute of Technology
Atlanta, Georgia

ABSTRACT

This paper presents the design and implementation of an advanced non-contact measurement system for metallic prismatic parts. In particular, these parts are Woodruff keys that are used heavily in the automotive industry. The metrology system developed is capable of measuring the maximum width and thickness of the keys using a six standard deviation tolerance on measurements to better than 200 μin and 0.002 in, respectively. This result is achieved via a combination of precision machine design, sensor calibration, and analog and digital signal processing. The system is considerably more accurate and less expensive than a number of metrology devices currently available on the market today. Furthermore in its current configuration, the measurement device is a powerful tool that can be used for both inspection as well as statistical process control.

1. INTRODUCTION

Woodruff keys are used in a wide variety of applications throughout industry. In particular, they are heavily used in the automotive industry to lock various parts together such as rotating shafts and pulleys. Historically, these keys have been manually inserted into position in an assembly line. However, with the advent of highly automated production lines, pneumatic assembly systems have begun to replace humans on the assembly line. Unfortunately to perform their task efficiently, these pneumatic key insertion devices require higher precision keys than their human predecessors. Figure 1 is a schematic of a typical key. Of particular concern is the fact that a burr at the end of the part can cause an automatic system to jam. This burr, which occurs infrequently, can yield a situation where a key costing 5-cents shuts-down a multi-million dollar line for 15-20 minutes.

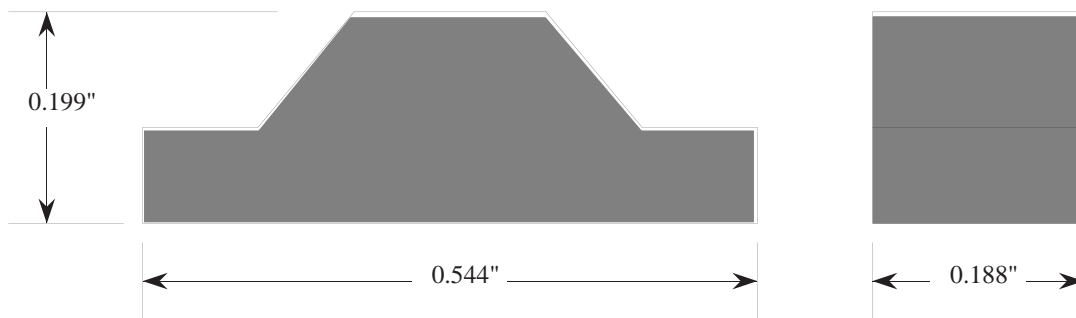


Figure 1. Typical Key Shape and Dimensions.

To this end, improved quality must be realized on the Woodruff keys; thus, a high speed and inexpensive measurement system must be developed. The objective of this system is two fold:

1. Perform statistical quality control on the keys as they are produced.
2. Identify and eliminate any keys that are out of specification.

While it is understood that the second objective may not fit into the mind-set of modern quality assurance practices, it is an objective that must be met until the process capability is improved to a point that out of specification keys do not adversely affect the production line.

The specifications for the inspection system are based on the tolerance levels required. The allowable deviation for a typical key is ± 0.003 in. on height, and ± 0.0005 in. on width. Since the shipment sizes for these parts are often greater than 50,000 pieces,

the minimum required inspection rate for this device is set at two parts per second so that practical time requirements can be maintained. Of course, considering the fact that these keys are produced in mass quantity and with relatively inexpensive equipment, the inspection device must be produced at minimal cost.

2. SYSTEM DESCRIPTION

A schematic of the system is shown in Figure 2. Keys are fed onto the gravity track from a vibrating feeder bowl and slide past the non-contact proximity sensors along the gravity track. The sensors are the eddy-current (inductive) type and provide a voltage proportional to the distance between the sensor and the surface of a metallic target. A 12 bit A/D board is used to capture signals from the sensors for processing in an MS DOS based computer. The computer utilizes this information for both process control statistics, and part defect status determination. Defective parts are ejected from the part stream by use of a solenoid actuated ejection gate. To obtain maximum resolution from the sensors, the gravity track is fabricated from high density polyethylene. This alleviates any interference with the electromagnetic fields of the sensors.

Two of the three inductive sensors are located above the surface of the gravity track and measure the proximity to the upper surface of the parts, as shown in Figure 2. These sensors are mounted in adjustable brackets so their positions can be changed to measure keys of various sizes. Electromagnetic interference between sensors, or cross-talk, is a significant problem when inductive sensors are placed in close proximity. Cross-talk reduces the accuracy of the sensors to a level that does not meet specifications for the inspection system. Thus, the sensors are staggered along the length eliminating cross-talk.

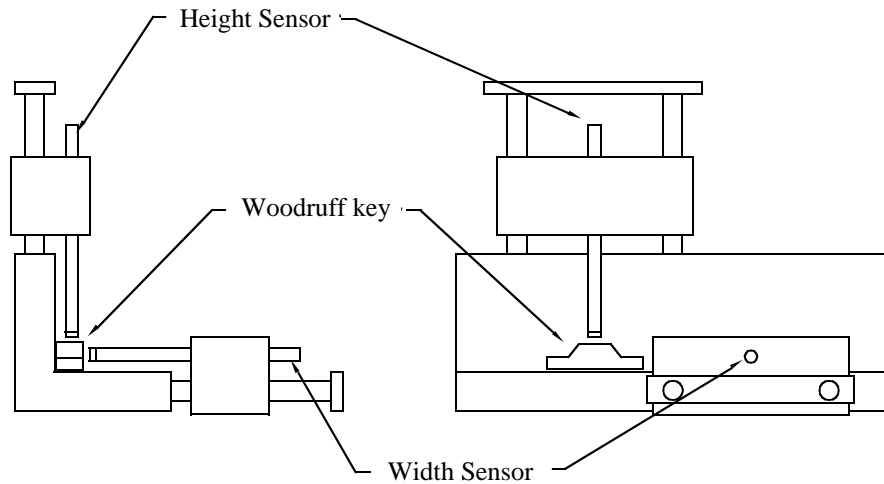


Figure 2. Sensor Arrangement Relative to the Gravity Track.

2.1. Reducing Measurement Sensitivity to Part Position Variation

Since a gravity track is employed as the part feeding mechanism for the system, the position of the part with respect to the sensors varies in a stochastic manner. Because of dirt and the high rate of travel down the track, the keys tend to bounce down the track. This leads to two types of variations in key position, normal and lateral to the eddy-current sensors. Clearly, part deviation normal to the sensors will yield incorrect measurement results as the basis of the measurement is the air-gap between the part and the sensor. Thus, if the part bounces closer to the sensor, it will appear to be larger than it actually is. Variations in the key's lateral position with respect to the sensor causes variations in the sensor field sector that is absorbed by the key. By interacting with different portions of the sensor field, slightly varying readings may be generated as the keys pass by the sensors. This generates repeatability problems with for the system. By the appropriate analysis and design measures, the bulk of these errors can be eliminated.

The first design modification to the system is the addition of an Ultra High Molecular Weight (UHMW) Polyethelene coating to the track. UHMW is particularly well suited for this application since its composite coefficient of friction with the keys is relatively low, and the UHMW is highly wear resistant. This design modification substantially reduces part vibration along the track; however, it does not completely eliminate the problem. Thus, further system enhancements are necessary.

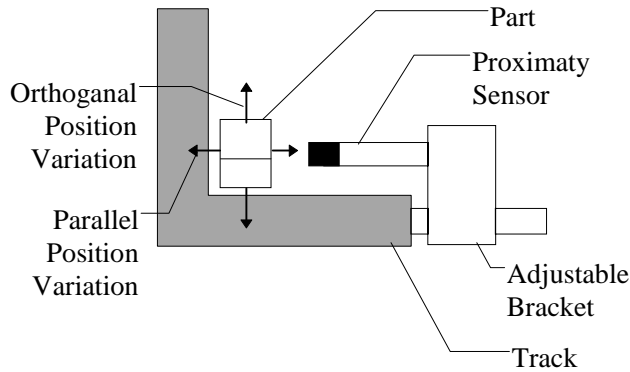


Figure 3. Variations in Part Position During Measurement.

Position variations parallel to the measurement axis are eliminated from the measurements by the use of a differential sensor arrangement. An additional sensor, located directly opposite the primary sensor is threaded into the bottom of the track as shown in Figure 4. The objective of the secondary sensor is to measure the location of the key underside with respect to the surface of the track. Although this sensor is located in the gravity rack, it does not penetrate the UHMW coating. Thus, the sliding motion of the key is not affected. The use of directly opposing sensors as shown in Figure 4 can result in cross-talk errors. However, during critical measurements the key shields the sensors from each other (Dufour et al., 1994). Unfortunately, field leakage around the keys during in-line measurement generates some cross-talk. This problem is eliminated simultaneously with the lateral positional error problem and is discussed below.

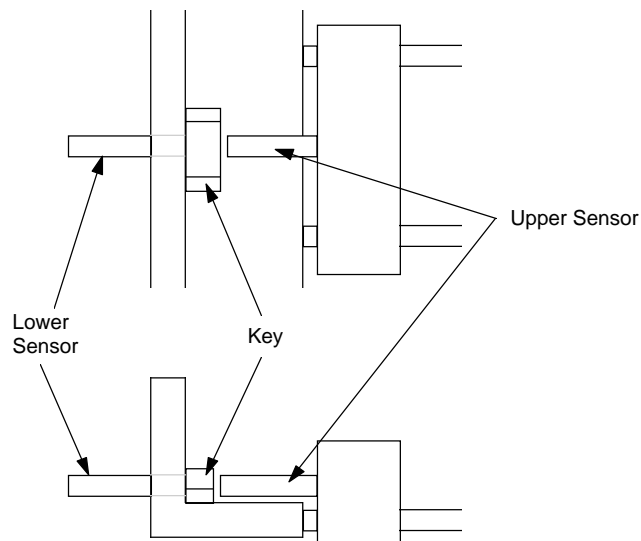


Figure 4. Differential Width Measurement.

The measurement is also affected by position variation orthogonal to the axis of measurement. As the key moves in an orthogonal fashion with respect to the sensor's magnetic field, it absorbs different segments of the field. This results in non-repeatable measurements since the density of the sensor's field varies with orthogonal position (the densest field being located at the center of the sensor tip Sykulski and Stoll, 1992). Using the appropriately designed conductive aluminum shielding as shown in Figure 5, sections of the field above and below the key position were impeded, eliminating sections of the field. Thus, the entire field is absorbed by the target key regardless of the bouncing motion of the key as shown in Figure 5. The shielding also has the effect of preventing field leakage over the key. This eliminates all cross-talk problems.

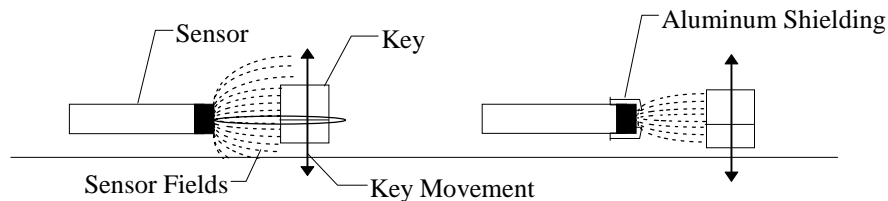


Figure 5. Use of Shielding to Reduce Measurement Variation.

It is critical to note that the eddy-current sensors are placed directly in-line with the dimension being measured, thus Abbe's principle is obeyed (Bryan, 1989). Furthermore, the in-line configuration of the sensors eliminates any errors generated by non-simultaneous measurement of opposing key surfaces. Two different errors can occur by non-simultaneous measurements. The first error is that the key may bounce and have different apparent heights. Thus, not having the sensors in line defeats the purpose of the second sensor. Secondly, since the key velocity is not constant with respect to time it is not possible to precisely related the two sensor readings to specific locations along the part. Without this relationship, a true maximum dimension cannot be determined.

3. SIGNAL PROCESSING

While mechanical design and instrumentation play a critical role in the measurement system's performance, it is the signal processing, both analog and digital, that permits the system to reach its ultimate repeatability and accuracy. This section briefly presents critical issues that were addressed in the system design and realization. Signal processing is divided into two distinct tasks: anti-alias analog filtering and digital noise attenuation filtering. It is important to note that due to the high precision nature of

this system, all of the filters must be completely modeled and calibrated. If an incorrect model is used to represent a particular filter the resulting errors (even if small) can yield errors on the order of 50 μin which are unacceptable for this application.

Although the gravity track simplifies the fabrication, operation and maintenance of the system, it substantially complicates its measurement and signal processing tasks due to inconsistent key velocity. Based on a large number of experimental trials it has been determined that the key velocity can deviate by more than $\pm 25\%$ from nominal. These significant deviations must be considered when sampling the sensors and converting the keys' spatial profile signature into the time domain. To demonstrate this, three sets of key data are plotted versus sample time in Figure 6. All three sets originate from the same key scan, but two of the sets have been modified to simulate different key speeds. The solid line indicates the sensor values as they were read while a measurement was performed. The dashed line and dotted line represent the key traveling with velocities of 25% above nominal and 25% below nominal, respectively.

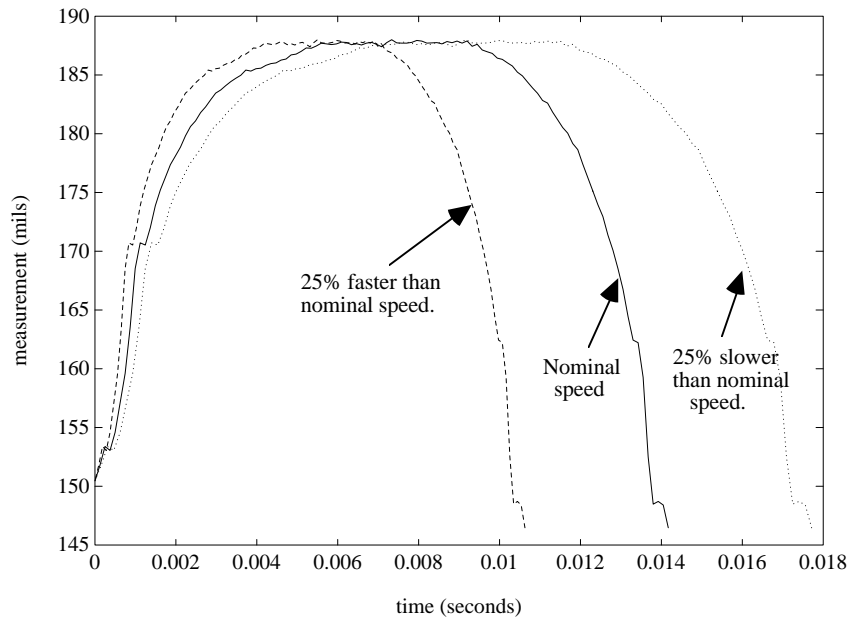


Figure 6. Effects of Key Velocity Variations on Measurement.

The frequency spectrum of these signals can be examined by performing a Fourier analysis on the data shown in Figure 6. A graph showing the magnitude of the relative frequency components of these variable-velocity key readings is presented in Figure 7. Clearly, keys traveling faster have significant components at higher frequencies than

those traveling at lower velocities. As the key velocity varies, the frequency spectrum of the resulting signal also varies. In order to meet the repeatability requirements, all filters must be extremely flat across the entire spectrum of the all samples regardless of velocity. If the filters are not flat, then attenuation or amplification of different frequencies, generated by varying velocities, will yield non-repeatable measurements for the system resulting in a failure to meet specifications. In fact, this entire system was fabricated and tested and did not meet specifications before the signal processing issues discussed in this section were addressed. Thus, signal processing can have a strong influence on the overall accuracy that the system can achieve, and if not properly understood can cause significant errors.

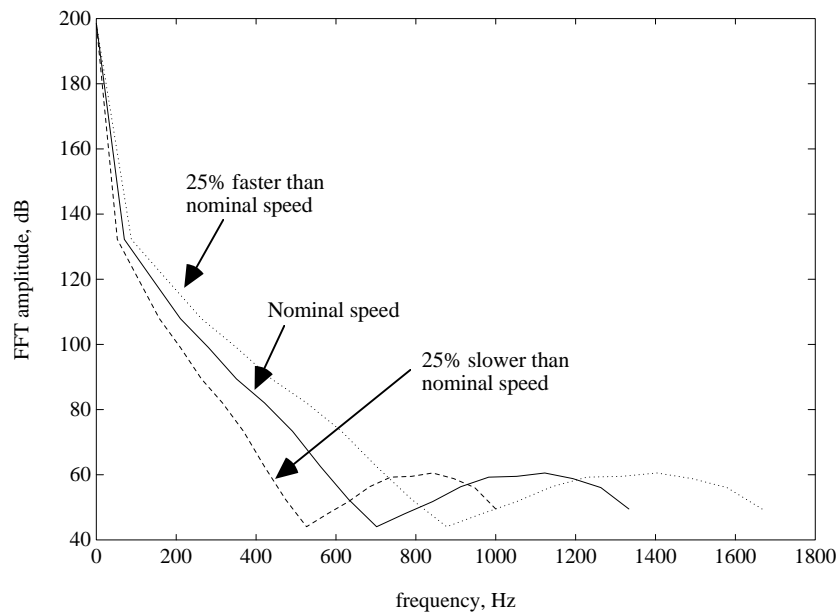


Figure 7. Frequency Domain Representation of Data with Varying Key Velocity.

3.1. Analog Anti-Alias Filters

The purpose of the anti-alias filter is to prevent aliasing by attenuating any frequencies that may exist above the Nyquist frequency, defined to be one half the sample rate. The sample rate for this application is specified by the requirement to obtain two hundred measurement points along the length of the key. Acquiring this many data points ensures that the peak values of the height and width are obtained. With a nominal key speed of 45 in./s, and a nominal key length of 0.544 in., the appropriate sample rate is given by

$$\left(\frac{1 \text{ key}}{0.544 \text{ in}}\right)\left(\frac{200 \text{ samples}}{1 \text{ key}}\right)\left(\frac{45 \text{ in}}{1 \text{ sec}}\right) = 16544 \text{ samples / sec} \quad (1)$$

The system is programmed to determine the appropriate sample rate as part of the system's calibration procedure, given sensor data from a series of calibration runs. From Equation (1), the Nyquist frequency is 8.3 kHz. A sample rate of 12 kHz was assumed for the purpose of analog filter design in order to include a reasonable factor of safety.

The cut-off frequency of the filters must be high enough to preserve the significant frequencies of the measurement, but still effectively eliminate noise and prevent aliasing. Examining the spectrum graphs of Figure 7, in conjunction with the system specifications, the spectrum components that are of interest lie below 800 Hz. The relative amplitudes of the frequencies are computed using a discrete Fourier transform and graphed using the Welch method of power spectrum estimation (Oppenheim et al., 1975). Based on this analysis, the filters are to be designed with a cut-off frequency of 2000 Hz. Because of their maximally flat response below the cut-off frequency, Butterworth configurations were used for both the digital and analog filters. Sixth order Butterworth filters, which have a roll-off rate of -120 dB per decade, are used as analog filters. With a cut-off frequency of 2000 Hz, signals at 6000 Hz are attenuated by a factor of 0.016. The analog filters were fabricated via cascading several Sallen-Key low-pass filters (Franco, 1988).

Precision components (*e.g.*, resistors) were used in the filter construction to match the actual filter performance as closely as possible to the target theoretical response. However, due to the fact that the capacitances and resistances of the actual components may deviate slightly from those specified in the design, the actual filter response must be experimentally validated. This verification is necessary since component deviations may lead to a filter with gain variations within the pass-band spectrum that yield unacceptable measurement error. Thus, the filters were assembled and their frequency response verified using a signal generator and an oscilloscope. (Note that the phase shift effects of this filter are not significant to its performance for this application. The phase shift's only effect is to create an insignificant delay in the data processing. Thus, it is not addressed in the system design.)

3.2. Digital Filter Design

Once frequency components above the Nyquist frequency have been removed by the analog filters, digital filters are then used to eliminate other frequency components

that are undesirable or of no use. Since the digital filter is simply the application of an equation, its performance is always ideal; thus, no special testing of the digital filters is required. However to eke out the absolute best performance from the system, careful consideration must be given to the filter design and implementation.

The design process for the digital filter is based on analog prototypes, using the bilinear transformation to obtain the discrete equivalent from the transfer function. (Tretter, 1976) The discrete filter is implemented recursively on the data, directly from the transfer function. The bilinear transformation, mapping the s-domain into the z-domain, is given as

$$s = \frac{z - 1}{z + 1} \quad (2)$$

Use of the bilinear transform has the effect of warping the frequency response of the digital transfer function. When the transfer function is converted into the z-domain (or, as the filter is transformed from an analog design to a digital realization), responses at frequencies of interest (*e.g.* the cut-off frequency) shift frequency slightly as a result of this warping. Typically, the effects of frequency warping are negligible. However, due to the high precision of this application coupled with the varying key velocities, frequency warping cannot be tolerated. To counter this effect, the cut-off frequency is pre-warped by

$$\Omega = \tan\left(\frac{\omega T}{2}\right) \quad (3)$$

Where ω is the desired cut-off frequency (rad/sec), T is the delay time between samples (sec), and Ω is the prewarped frequency to be used in the analog filter design (rad/sec).

The first step of the filter design is to determine the order of filter to be implemented. Higher order filters allow faster roll-off rates above the cut-off frequency. Though higher order digital filters do not increase the potential for noise in the system (as high order analog filters do), they do require more computer processing time. (Lorenz and Schade, 1986) Processing time is important due to the real time nature of this application. For each key, a 200 element array must be filtered digitally, requiring the computation of the difference equation of the digital filter for each array element. A fourth order Butterworth filter has a roll-off rate of 80 dB/decade, which is sufficient for this application and demands computing capabilities that do not substantially tax the system. The pre-warped frequency for the analog version of this filter design is given by

$$\Omega = \tan\left(\frac{\omega T}{2}\right) = \tan\left(\frac{\omega_s T}{12}\right) = \tan\left(\frac{2\pi\omega_s}{12\omega_s}\right) = \tan\left(\frac{\pi}{6}\right) = 0.577 \quad (4)$$

where ω_s is the sample frequency (12 kHz). The transfer function for a fourth order analog Butterworth filter with a cut-off frequency of 0.577 rad/sec, is

$$\frac{Y(s)}{X(s)} = \frac{0.111}{s^4 + 1.51s^3 + 1.14s^2 + 0.502s + 0.111} \quad (5)$$

where $X(s)$ and $Y(s)$ are the filter input and output, respectively. Using the bilinear transform given by equation (2) and simplifying terms, equation (5) is mapped into the z-domain as

$$\frac{Y(z)}{X(z)} = \frac{0.026 + 0.104z^{-1} + 0.156z^{-2} + 0.104z^{-3} + 0.026z^{-4}}{1 - 1.31z^{-1} + 1.03z^{-2} - 0.363z^{-3} + 0.0559z^{-4}} \quad (6)$$

Equation (6) can easily be transformed into the difference equation that is implemented on the system.

The final step in the digital filter implementation is to initialize its state at the beginning of each key scan. To set the initial conditions, the first four points in the digitally filtered array are set equal to the sample data output from the analog filters. Due to the small time constant of the digital filter, any error created by this initialization approximation is insignificant since the peak value is not encountered until a significant number of data points have been processed. This permits any transients from the filter initialization to decay well before critical measurements are processed.

4. SYSTEM CALIBRATION

Before the system can achieve target specifications, each sensor must be properly calibrated. Without proper calibration, measurements produced by the system would be of little value. Due to the fact that this system is intended to operate in a production environment, the calibration procedures must be simple and quick. This permits the fast and error-free calibration that is needed to address issues such as thermal drift and material property fluctuations. This section briefly describes the calibration procedure that is a key part of the functionality of the system and provides it with substantial flexibility and ease of use. The discussion is limited to the sensors used to measure the key width in a differential configuration. The calibration for the single sensor measuring height is similar in nature, although slightly less involved.

Although eddy-current probes are non-linear over their entire operational displacement range (± 0.025 in), they are quite linear over the application range of ± 0.005 in. Within this small range, the relationship between sensor voltage and distance to target is fairly linear, thus two calibration values (slope and offset at a specified nominal target distance) are required (Slocum, 1992). Also these sensors are extremely stable, with respect to calibration, when only a small fraction of the total sensor depth-of-field is utilized.

H_m	Key height measurement (in)
W_m	Key width measurement (in)
H_n	Nominal key height (in)
W_n	Nominal key width (in)
VS_{nl}	Lower sensor voltage, calibration (nominal) key measurement (V)
VS_{nu}	Upper sensor voltage, calibration (nominal) key measurement (V)
VS_{ml}	Lower sensor voltage, inspected key measurement (V)
VS_{mu}	Upper sensor voltage, inspected key measurement (V)
SS_u	Upper sensor slope (in/V)
SS_l	Lower sensor slope (in/V)

Table 1. Nomenclature for Calibration Variables.

The output of the probes is a voltage in the range of 0-10 V that is proportional to the distance to the target part. Higher voltages indicate larger distances. Given proximity measurements from both in line sensors used for differential width measurement, the width of the key is given by

$$W_m = W_n + SS_u * (VS_{nu} - VS_{mu}) + SS_l * (VS_{nl} - VS_{ml}) \quad (7)$$

(Note, a similar equation is used for the key height calculation except measurements from a second sensor are not included in the height calculation. Thus, the lower sensor voltages would be set to zero for the height measurement.)

The sensors' voltage/displacement slope is dependent on key geometry and material. For the differential width measurement, one slope per sensor must be determined. In order to properly compute the voltage vs. displacement characteristics for width measurement, calibration keys were manufactured by removing material from keys of nominal thickness. Keys widths were reduced by precisely machining 0.002 in and 0.0005 in from a set of calibration keys. The upper width sensor is then positioned to the operating point, (the lower width sensor is stationary since it is threaded into the bottom of the track), the calibration keys, including a key of nominal width, are repeatedly fed

through the gravity track for 100 passes. The raw sensor data obtained are matched to the appropriate key width as measured by a micrometer, and a least-squares linear regression is employed to determine the unknown constants in equation (7). (The slope of the height sensor is determined by adjusting sensor position while measuring the specific keys. Sensor position change is measured with a micrometer while the computer displays the digitized sensor output on the screen.)

5. RESULTS

Figure 8 displays a plot of the data collected from the width calibration analysis showing three distinct data clouds for the three different keys employed. From this chart, it is straightforward to visualize how differential measurement decreases variation in readings. The accuracy of single sensor measurements is demonstrated by the projection of an individual data cloud onto the horizontal axis. Given only the upper sensor readings, the distinction cannot be made between the key which is 0.188 in. thick (the nominal size) and the out-of-specification key that is 0.1875 in. thick. The differential accuracy is given by the width of each data cloud along the line fit to those data. This width indicates a 6σ accuracy of 200 $\mu\text{in.}$ From this analysis, the bottom sensor has a slope of approximately 547 V/in., and the top sensor has a slope of approximately 431 V/in.

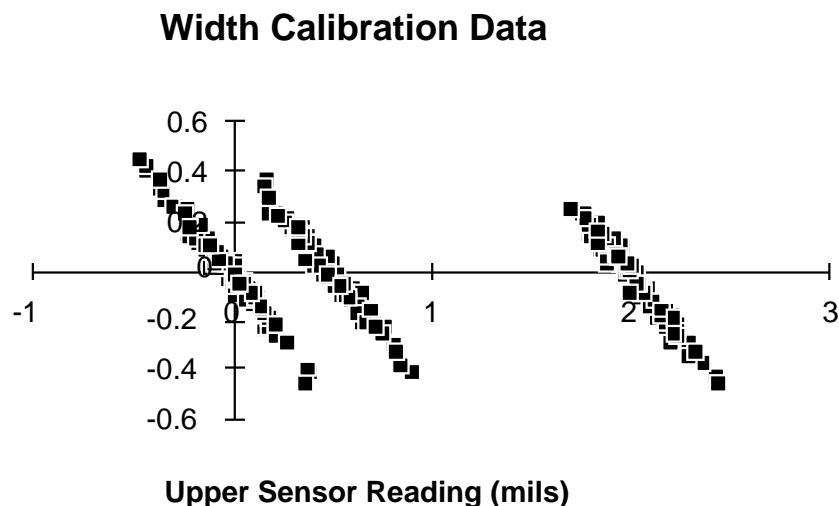


Figure 8. Calibration of the Differential Width Sensors.

After initial calibration, the system was put into use inspecting keys. Based on its calibration data, it has met the specification of inspecting the maximum width and height

of Woodruff keys to a $\pm 3\sigma$ accuracy of 500 μin and 0.003 in, respectively, at a rate of 2 keys per second. The system is capable of inspecting the keys much faster than the keys can be fed from the feeder bowl. (Maximum key feed rates from an instrumentation and data processing perspective are approximately 110 parts per minute.) The system has a standard deviation of 230 μin on key height measurements (which employs only a single sensor), and a standard deviation of 34 μin on key width measurements (using the two sensors in a differential configuration).

6. CONCLUSIONS

This paper presented a high-speed, non-contact metrology system that has the following innovative properties:

1. Measurement standard deviation of 230 μin on key height.
2. Measurement standard deviation of 34 μin on key width.
3. Rapid and simple calibration procedure.
4. Low cost, utilizing of off-the-shelf components.

In order to achieve the system capabilities, the following areas of electro-mechanical system design were employed:

1. Precision system design and alignment.
2. Digital and analog filter design.
3. Effective calibration procedures for precision measurement.

It is the combination of these areas that resulted in this novel, precise and extremely cost-effective system.

This system has been assembled at a hardware cost of approximately seven-thousand dollars, including an AT bus computer, A/D board, inductive sensors, and feeder bowl. It is currently in operation and is capable of measuring parts at high speed with a repeatability and an accuracy comparable to that of typical micrometers.

This device has significant potential for other inspection applications. Although inductive sensors are economical they are limited to metallic targets. They are also sensitive to material characteristic variations from part to part. In addition, because of the limited depth of field and large measuring area, the measurements are restricted to peak values of width and height for the parts. However, there are a wide variety of other sensor that may be employed on the system. For example, optical sensors are available that can be used on non-metallic targets. Although considerably more expensive than inductive sensors, optical sensor technology has the capability of increased depth of field combined

with a sharper measurement target area. Using such sensors, more detailed information pertaining to the part profile may be collected and examined.

7. REFERENCES

1975, Oppenheim, A.V. and Schaffer, R.W., *Digital Signal Processing*, Prentice-Hall, pp. 556.

1976, S.A. Tretter, *Introduction to Discrete-Time Signal Processing*, John Wiley & Sons, Inc., NY, pp. 212-219.

1986, Lorenz, R. D., and Schade, D. K., "Synthesis of a High Speed Signal Processing System," IECON'86: 1986 International Conference on Industrial Electronics, Controls, and Instrumentation. pp. 657- 662.

1988, S. Franco, *Design with Operational Amplifiers and Analog Integrated Circuits*, McGraw-Hill, Inc., NY, pp. 122-123, 153-157.

1989, J. B. Bryan, "The Abbe Principle Revisited-An Updated Interpretation," *Precision Engineering*, Vol. 1, No. 3, pp. 129-132.

1992, A.H. Slocum, *Precision Machine Design*, Prentice Hall Inc., Englewood Cliffs, N.J., 1992, pp. 133-134, 247-253.

1992, Sykulski, J. K. and Stoll, R. L., "Magnetic Field Modeling and Calculation of Reflected Impedance of Inductive Sensors," *IEEE Transactions on Magnetics*, v 28, N. 2, pp. 1426-1429.

1994, Dufour, I., Busawon, M., Premel, D., and Placko, D., "General Analysis of Inductive Sensor Based Systems for Non- Destructive Testing," *Journal De Physique*, III, v. 4, n. 8, pp. 1481-1493.